Optimal control of multilevel quantum systems in the field-interaction representation

Praveen Kumar
Department of Physics, Stevens Institute of Technology, Hoboken, New Jersey 07030, USA
and Department of Chemistry and Biochemistry, Texas Tech University, Lubbock, Texas 79409, USA

Svetlana A. Malinovskaya
Department of Physics, Stevens Institute of Technology, Hoboken, New Jersey 07030, USA

Vladimir S. Malinovsky*
U.S. Army Research Laboratory, 2800 Powder Mill Road, Adelphi, Maryland 20783, USA
(Received 2 September 2014; published 29 September 2014)

A control strategy incorporating a fixed carrier frequency constraint on the optimal field is presented. As an illustrative example we consider the creation of maximum coherence in a six-level Λ system by solving the Schrödinger equation without the rotating-wave approximation in the field-interaction representation. We demonstrate that application of the optimal control theory optimization reformulated in the field-interaction representation allows one to keep the carrier frequency of the control field constant and successfully optimize off-resonant processes in multilevel quantum systems.

DOI: 10.1103/PhysRevA.90.033427 PACS number(s): 32.80.Qk, 33.80.Wz, 02.30.Yy, 03.67.Lx

I. INTRODUCTION

During the last few decades we have witnessed significant interest and advances in controlling atomic and molecular dynamics using shaped ultrafast laser pulses. Coherent control of quantum systems has found broad applications in atomic and molecular spectroscopy, laser-induced cooling, quantum optics, manipulation of chemical reactions and biological processes, as well as in quantum information [1–4]. Various experimental and theoretical methods have been developed to achieve a target quantum state in atomic and molecular systems, including stimulated Raman adiabatic passage (STIRAP) [2,5,6] and chirped-pulse excitation [7].

Optimal control theory (OCT) [8–12] is a control technique that is considerably more advanced mathematically. The OCT provides a powerful tool for the efficient manipulation of the quantum system to reach a desired objective at a given time by means of an optimized laser field, and it has been applied successfully to a broad variety of problems in physics and chemistry [13–20]. In order to design an optimal field, OCT requires the maximization or minimization of the field-dependent cost functional which usually incorporates the desired dynamical transformation that has to be achieved, and, in many cases, it contains a penalty term to minimize the field energy. An additional state-dependent penalty term can be incorporated into the cost functional if it is required to minimize the population of some unwanted states [5,6,20]. The field equations obtained in the variational OCT framework are solved numerically in an iterative fashion and analytically in some rare instances. Various numerical iterative methods have been used for the maximization or minimization of the cost functional [14]. The progress of the optimization depends on the choice of the initial guess field and the efficiency of the numerical iterative method; a large number of iterations are required for a bad guess of the field while progress is faster for a good guess of the field. The analysis of the optimal field and extracting control mechanism can be very challenging, depending on the complexity of the quantum system under investigation. However, the spectrum of the optimal field obtained using OCT always has major contributions corresponding to the resonance transition frequencies of the system, regardless of the initial choice of carrier frequency of the guess field [21]. This result can be explained by the presence of the field energy penalty term in the cost functional; this energy constraint makes a solution with minimal energy more favorable, since the resonant excitation is always more energy efficient than the off-resonant one.

In this paper, we propose an OCT algorithm incorporating a spectral constraint on the optimal control field. We test the performance of the method using an example of creating maximum coherence in the multilevel Λ system and focusing on the off-resonant excitation scenario. To address the desired constraints on the spectral characteristics of the optimal control field, which are defined by the laser setup parameters in an experiment, we modify the optimization procedure by solving the Schrödinger equation without the rotating-wave approximation (RWA) in the field-interaction representation [22]. The proposed strategy allows us to choose the spectral bandwidth in a controllable fashion and optimize only the external field envelopes while the central frequency of the control field is fixed. In contrast to earlier developed methods [23–27], the proposed optimization scheme does not require the use of a numerically expensive procedure of fast Fourier transformation in each iteration, while it makes it possible to incorporate realistic experimental constraints in computational pulse optimization.

The paper is organized as follows. In Sec. II we present the objective cost functional which must be maximized to obtain an optical field to achieve the desired optimization. The control field equations are derived using a penalty on the field energy and an additional penalty function to minimize the population of the excited intermediate state throughout the time evolution. Section III outlines the parameters of the quantum six-level Λ

*vsmalinovsky@gmail.com

system, gives a detailed description of the optimal control theory implementation using the Krotov method [28] for the creation of maximum coherence, and presents a strategy that incorporates the carrier frequency constraint on the optimal field. Finally, Sec. IV is the conclusion.

II. OPTIMAL CONTROL EQUATIONS

In this section we outline the OCT approach [8–12,21] to optimize an external field which drives an initial state $|\psi\rangle$ to a specified target state $|\phi\rangle$ at the final time $t = T$. From an optimal solution we require that the system wave function at the final time, $|\psi(T)\rangle$, should be as close as possible to the target state, $|\phi(T)\rangle$, i.e., the overlap $|\langle\psi(T)|\phi(T)\rangle|^2$ is maximal at time T. In order to obtain a control field equation with a realistic field amplitude we minimize the field energy by using a respective penalty. In addition, if it is desirable during the control process to suppress the transient population of some excited or intermediate states [5,6,14,29], one may introduce another penalty function, and use (as shown below) a projection operator $\hat{P} = |\psi_{\rm int}(t)\rangle\langle\psi_{\rm int}(t)| = \sum_k |k\rangle\langle k|$, where $|k\rangle$ is the eigenket of the unwanted state. To make sure that the wave function $|\psi(t)\rangle$ is satisfying the Schrödinger equation, the Lagrange multiplier function $|\chi(t)\rangle$ is used.

In general, the complete cost functional $J[\epsilon(t)]$, which must be maximized, is represented as a sum of the final time objective, the constraint over the field energy, the unwanted state constraint, and the dynamical part containing the Lagrange multiplier,

$$J[\epsilon(t)] = |\langle\psi(T)|\phi(T)\rangle|^2 - \frac{\alpha}{s(t)}\int_0^T dt[\epsilon(t)-\epsilon_r(t)]^2 - \beta\int_0^T dt\,\langle\psi(t)|\hat{P}|\psi(t)\rangle - 2\,\mathrm{Re}\left[\int_0^T dt\,\langle\chi(t)|\,\frac{\partial}{\partial t}+\frac{i}{\hbar}\hat{H}\,|\psi(t)\rangle\right], \quad (1)$$

where α is the penalty parameter which defines the significance of the field energy, $s(t)$ denotes the shape function to smoothly switch the field on and off (to ensure an experimentally feasible profile of the laser pulse), $\epsilon_r(t)$ denotes a reference field [$\epsilon_r(t) = 0$ corresponds to a common choice of minimizing the field energy], and β is the penalty parameter for the unwanted state population. The optimization procedure can be controlled by the value of α: A small value results in a small weight of the field energy and allows for large modifications of the field, while a large value of α represents a conservative search strategy, allowing only small modifications of the field during each iteration.

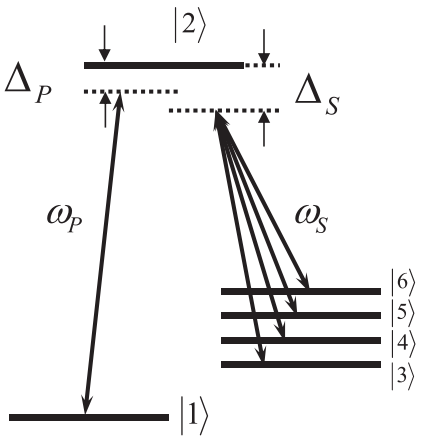

FIG. 1. Schematic of a six-level Λ system.

Taking variations of the cost functional with respect to $|\chi(t)\rangle$, $|\psi(t)\rangle$, and $\epsilon(t)$ leads to the following set of control equations,

$$i\hbar\frac{\partial}{\partial t}|\psi(t)\rangle = \hat{H}|\psi(t)\rangle, \quad (2)$$

$$\frac{\partial}{\partial t}|\chi(t)\rangle = -\frac{i}{\hbar}\hat{H}|\chi(t)\rangle + \beta\hat{P}|\psi(t)\rangle, \quad (3)$$

$$\epsilon(t) = \epsilon_r(t) + \frac{s(t)}{\alpha\hbar}\mathrm{Im}\,\langle\chi(t)|\,\frac{\partial\hat{H}}{\partial\epsilon(t)}\,|\psi(t)\rangle\,, \quad (4)$$

and variation with respect to $|\psi(T)\rangle$ provides the initial condition for the Lagrange multiplier, $|\chi(T)\rangle = |\phi(T)\rangle\langle\phi(T)|\psi(T)\rangle$. Equations (2) and (3) determine the time evolution of the system wave function and the Lagrange multiplier, which are used in Eq. (4) to determine the optimal field providing the maximum of the overlap $|\langle\psi(T)|\phi(T)\rangle|^2$.

As an example, we consider an implementation of the general OCT formalism to a six-level Λ-type system shown in Fig. 1; the pump field with carrier frequency ω_P couples the initial state $|1\rangle$ and an intermediate state $|2\rangle$, while the Stokes field with carrier frequency ω_S couples the intermediate state $|2\rangle$ to the rest of the states $|3\rangle$–$|6\rangle$. Our goal here is to design the pump and Stokes pulses which provide a maximal coherent superposition of the ground state $|1\rangle$ and the adjacent states $|4\rangle$ and $|5\rangle$ while the population of the intermediate state $|2\rangle$ and the two other states $|3\rangle$ and $|6\rangle$ is minimized.

In the field-interaction representation [22], the system wave function $|\psi(t)\rangle = \sum_{i=1}^{6} a_i(t)|i\rangle$, where $a_i(t)$ is the probability amplitude to be in state $|i\rangle$, is governed by the Schrödinger equation with the Hamiltonian of the form

$$\hat{H} = -\frac{\hbar}{2}\begin{pmatrix} 2\Delta_P & W_P(t) & 0 & 0 & 0 & 0 \\ W_P^*(t) & 0 & W_S^*(t) & W_S^*(t) & W_S^*(t) & W_S^*(t) \\ 0 & W_S(t) & 2(\Delta_S+\delta) & 0 & 0 & 0 \\ 0 & W_S(t) & 0 & 2\Delta_S & 0 & 0 \\ 0 & W_S(t) & 0 & 0 & 2(\Delta_S-\delta) & 0 \\ 0 & W_S(t) & 0 & 0 & 0 & 2(\Delta_S-2\delta) \end{pmatrix}, \quad (5)$$

where $W_{P,S}(t) = \Omega_{P,S}(t)(1 + e^{-2i\omega_{P,S}t})$, $\Omega_{P,S}(t) = \mu_{ij}E^0_{P,S}(t)/\hbar$ are the pump and Stokes Rabi frequencies, μ_{ij} are the dipole moments, and $E^0_{P,S}(t)$ are the envelopes of the pump and Stokes pulses, $\Delta_{P,S} = \omega_{P,S} - \omega_{21,24}$ are the single-photon detuning of the pump and Stokes carrier frequency $\omega_{P,S}$ from the respective transition frequency $\omega_{21,24}$, and spacing in the four-level manifold is $\omega_{34} = \omega_{45} = \omega_{56} = \delta$.

For the Lagrange multiplier vector $b_i(t)$, probability amplitudes $a_i(t)$, and the Rabi frequency envelopes $\Omega_{P,S}(t)$, Eqs. (2)–(4) take the following forms,

$$i\hbar\frac{\partial a_i(t)}{\partial t} = \hat{H}_{ij}a_j(t), \tag{6}$$

$$\frac{\partial b_i(t)}{\partial t} = -\frac{i}{\hbar}\hat{H}_{ij}b_j(t) + \beta a_2(t)\delta_{i2}, \tag{7}$$

$$\Omega_P(t) = \Omega^r_P(t) - \frac{s(t)}{2\alpha\hbar}\mathrm{Im}[b^\star_1(t)(1 + e^{-2i\omega_P t})a_2(t) + b^\star_2(t)(1 + e^{2i\omega_P t})a_1(t)], \tag{8}$$

$$\Omega_S(t) = \Omega^r_S(t) - \frac{s(t)}{2\alpha\hbar}\mathrm{Im}[b^\star_2(t)(1 + e^{2i\omega_S t})a_3(t) + b^\star_2(t)(1 + e^{2i\omega_S t})a_4(t) + b^\star_2(t)(1 + e^{2i\omega_S t})a_5(t) + b^\star_2(t)(1 + e^{2i\omega_S t})a_6(t)$$
$$+ b^\star_3(t)(1 + e^{-2i\omega_S t})a_2(t) + b^\star_4(t)(1 + e^{-2i\omega_S t})a_2(t) + b^\star_5(t)(1 + e^{-2i\omega_S t})a_2(t) + b^\star_6(t)(1 + e^{-2i\omega_S t})a_2(t)], \tag{9}$$

where $\Omega^r_{P,S}(t)$ are the reference pump and Stokes Rabi frequencies.

III. NUMERICAL RESULTS AND DISCUSSION

To achieve our optimization goal, we solve Eqs. (8) and (9) for pump and Stokes Rabi frequencies using the iterative Krotov method [14,28]. As an initial guess, we use the Gaussian form for the pump and Stokes Rabi frequencies, $\Omega_{P,S}(t) = \Omega_0 \exp[-(t - T_c)^2/2\tau_0^2]$, where $\Omega_0 = 0.05$ fs^{-1}, $\tau_0 = 125$ fs, and $T_c = 500$ fs, and the target time is equal to $T = 1$ ps. We consider the two-photon resonant excitation scheme, with the single-photon detunings $\Delta_P = \Delta_S = 0.1$ fs^{-1}; the transition frequencies are chosen to be $\omega_{21} = 0.517$ fs^{-1}, $\omega_{24} = 0.375$ fs^{-1}, and spacing in the four-level manifold is $\omega_{34} = \omega_{45} = \omega_{56} = 0.02$ fs^{-1}. The time-dependent Schrödinger equation, Eq. (6), and the inhomogeneous equation for the Lagrange multiplier vector, Eq. (7), are solved without the rotating-wave approximation. Neglecting the relative phase relations between the probability amplitudes a_i in the target wave function, we chose the population distribution ($|a_1|^2 = |a_4|^2 = |a_5|^2 = 1/3, |a_2|^2 = |a_3|^2 = |a_6|^2 = 0$) as the target of the optimization procedure.

The optimized results obtained for the off-resonant excitation ($\Delta_{P,S} = 0.1$ fs^{-1}), with and without a penalty on the intermediate excited-state population, are presented in Figs. 2 and 3. The target state populations ($|a_{1,4,5}|^2$) are shown by solid lines, while the transient population of other states is shown by the dashed lines. Optimized pump and Stokes Rabi frequency envelopes and populations are obtained

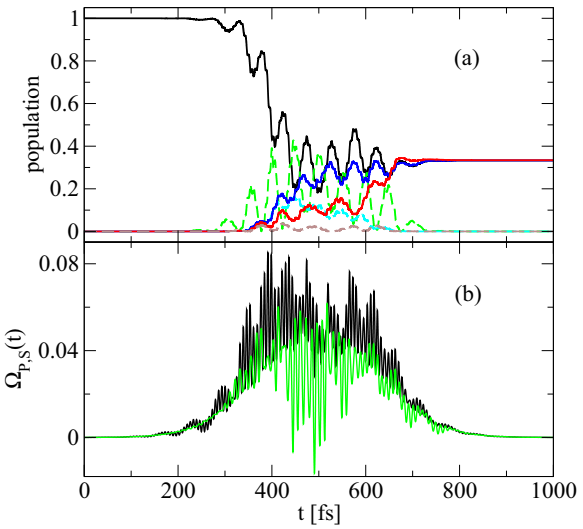

FIG. 2. (Color online) Population dynamics in the six-level Λ system optimized without a penalty on the second state population. (a) The population of the target states is shown by solid lines: $|1\rangle$ (black), $|4\rangle$ (blue), $|5\rangle$ (red); the transient population of other states is shown by dashed lines: $|2\rangle$ (green), $|3\rangle$ (cyan), and $|6\rangle$ (brown). (b) The optimal pump (black line) and Stokes (green line) Rabi frequencies.

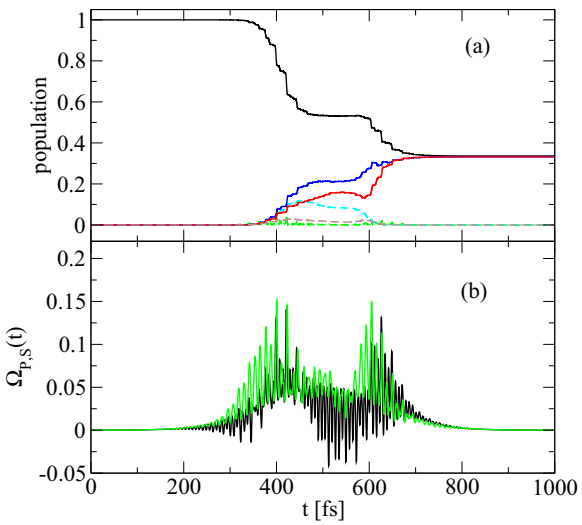

FIG. 3. (Color online) Population dynamics in the six-level Λ system optimized with a penalty on the second state population. (a) The population of the target states is shown by solid lines: $|1\rangle$ (black), $|4\rangle$ (blue), $|5\rangle$ (red); the transient population of other states is shown by dashed lines: $|2\rangle$ (green), $|3\rangle$ (cyan), and $|6\rangle$ (brown). (b) The optimal pump (black line) and Stokes (green line) Rabi frequencies.

after 5000 iterations in both cases (Figs. 2 and 3). However, the transition probability defined as $\mathcal{P} = |\langle\psi(T)|\phi(T)\rangle|^2$ and the optimized cost functional $J[\epsilon(T)]$ reaches nearly 100% after only a few iterations. We observe that, independently on the value of the penalty parameter on the intermediate excited-state population, we successfully obtain the maximum coherences $|\varrho_{14}| \approx |\varrho_{15}| \approx 1/3$ at the target time $T = 1$ ps, here $\varrho_{ij} = a_i^* a_j$.

The amplitudes of the pump and the Stokes Rabi frequencies are modulated in time, which is shown by fast oscillations in Figs. 2(b) and 3(b). This amplitude modulation splits the excitation fields so that the pump and the Stokes fields contain several subpulses (we will discuss this point in more detail later in the text). Overall, more intense pulses are required for the constrained optimization [Fig. 3(b)] in comparison to the unconstrained optimization [Fig. 2(b)]—this is due to a penalty on the state $|2\rangle$ population.

When the population of the intermediate state is not penalized, we observe sequential population transfer from the ground state $|1\rangle$ to the excited state $|2\rangle$ and then from $|2\rangle$ to the target states $|4\rangle$ and $|5\rangle$ [Fig. 2(a)]. At an earlier time, we observe a few Rabi oscillations between states $|1\rangle$ and $|2\rangle$; the population of the second state reaches about 40%. Sequential population transfer can be explained by the intuitive pulse sequence: The pump pulse precedes the Stokes pulse, and the pump field is a bit stronger [see Fig. 2(b)].

By applying a penalty on the second state population we impose suppression of the transient population in this state, which results in a different solution of the optimization procedure: The structure of the optimal control fields resembles the counterintuitive pulse sequence [see Fig. 3(b)]. The transient second state population is now substantially reduced, with a maximum value of a few percent. It is well known that the second state population suppression can be successfully accomplished using a counterintuitive pulse sequence, when the Stokes pulse precedes the pump pulse, as in the STIRAP scheme [2]. That time-delay feature can clearly be seen in the pulse sequence shown in Fig. 3(b); moreover, the Stokes field is more intense in this case.

The demonstrated differences in the population dynamics and in the observed control field structures reveal clearly the influence of the excited-state population constraint on the optimization procedure and the optimal results of the OCT implementation.

The spectra of the pump and the Stokes fields are shown in Fig. 4(a). The pump spectrum shown by the black line in Fig. 4(a) has a major frequency structure at about 0.417 fs^{-1} corresponding to the pump carrier frequency. The Stokes spectrum shown by the gray (green online) line in Fig. 4(a) has major peaks at 0.275 fs^{-1} corresponding to the Stokes central frequency. There are some additional extra peaks which are clearly artificial components related to the iterative optimization procedure and to the presence of the fast oscillating terms in the Hamiltonian. These detrimental spectral components are not essential for control and can be easily suppressed without considerable change in the time-dependent control fields and degradation of the desired system dynamics. By applying a simple (unit step function) filter mask we remove these extra frequency peaks. The allowed frequency range is chosen as $\omega \in [0.25,0.6]$ and $\omega \in [0.1,0.45]$ for the pump and the Stokes fields, respectively. The modified field spectra are presented in Fig. 4(b). By making the inverse Fourier transformation to the time domain, we obtained modified fields [see Fig. 5(b)] and solve the time-dependent Schrödinger equation.

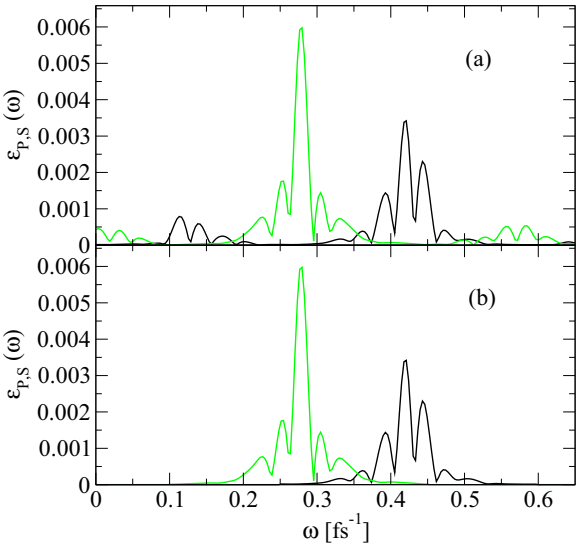

FIG. 4. (Color online) Spectra of the pump (black line) and Stokes (green line) pulses: (a) Optimized fields corresponding to the results presented in Fig. 3. (b) Modified fields after filtering as discussed in the text.

Figure 5(a) shows the population dynamics under control by the filtered fields. As we see, the dynamics of the state amplitudes is very similar to the optimal control solution presented in Fig. 3(a). There is some discrepancy in the target state populations of a few percent order, which is related to

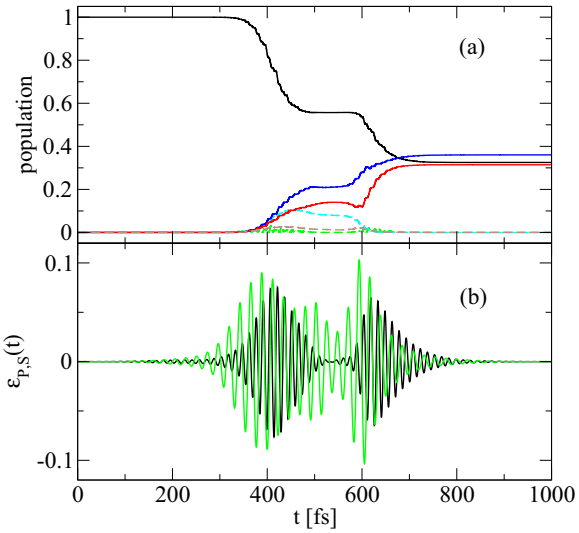

FIG. 5. (Color online) Population dynamics in the six-level Λ system. (a) The population of the target states is shown by solid lines: $|1\rangle$ (black), $|4\rangle$ (blue), $|5\rangle$ (red); the transient population of other states is shown by dashed lines: $|2\rangle$ (green), $|3\rangle$ (cyan), and $|6\rangle$ (brown). (b) The pump (black line) and Stokes (green line) fields obtained by filtering extra frequencies in the optimized solution.

the numerical realization of the fast Fourier transformation. The modified control fields in Fig. 5(b) show clearly the two-subpulse structure and the counterintuitive pulse sequence, as we mentioned above.

IV. CONCLUSION

We have proposed a modification of the OCT technique to control the dynamics of the multilevel wave function by optimizing the external field envelope. The presented strategy keeps the main ingredients of the well-established OCT methodology, including a penalty on the field energy and on the unwanted state population, while the dynamical part of the optimization procedure is treated in the field-interaction representation. In this way, we find the optimal field envelope and keep the carrier frequency of the control field constant, meaning that we have complete freedom to define the central frequency of the optimal field. We have demonstrated a successful implementation of the scheme by considering the creation of a maximum coherence in the six-level Λ system using off-resonant external control fields. Note that our method does not require the use of a spectral filtering constraint in the cost functional (which is usually implemented by applying a numerically expensive procedure of forward and backward fast Fourier transformation in each iteration), while it makes it possible to incorporate realistic experimental constraints in the computational pulse optimization. We believe that the proposed modification of the OCT strategy provides a useful tool to control the central frequency in the iterative optimization and can facilitate future applications of the optimal control methods in experiments.

ACKNOWLEDGMENTS

The authors thank Ignacio R. Sola for valuable discussions. This research was supported in part by the National Science Foundation under Grants No. PHY11-25915 and No. PHY12-05454.

[1] T. Kamiya, F. Saito, O. Wada, and H. Yajima, *Femtosecond Technology* (Springer, Berlin, 1999).
[2] K. Bergmann, H. Theuer, and B. W. Shore, Rev. Mod. Phys. **70**, 1003 (1998).
[3] P. Král, I. Thanopulos, and M. Shapiro, Rev. Mod. Phys. **79**, 53 (2007).
[4] D. M. Reich, G. Gualdi, and C. P. Koch, Phys. Rev. Lett. **111**, 200401 (2013).
[5] I. R. Sola, V. S. Malinovsky, and D. J. Tannor, Phys. Rev. A **60**, 3081 (1999).
[6] V. Kurkal and S. A. Rice, J. Phys. Chem. B **105**, 6488 (2001).
[7] L. P. Yatsenko, B. W. Shore, T. Halfmann, K. Bergmann, and A. Vardi, Phys. Rev. A **60**, R4237 (1999).
[8] S. A. Rice and M. Zhao, *Optical Control of Molecular Dynamics* (Wiley, New York, 2000).
[9] M. Shapiro and P. Brumer, *Principles of the Quantum Control of Molecular Processes* (Wiley, New York, 2003).
[10] G. G. Balint-Kurti, S. Zou, and A. Brown, Adv. Chem. Phys. **138**, 43 (2008).
[11] R. Kosloff, S. A. Rice, P. Gaspard, S. Tersigni, and D. J. Tannor, Chem. Phys. **139**, 201 (1989).
[12] A. P. Peirce, M. A. Dahleh, and H. Rabitz, Phys. Rev. A **37**, 4950 (1988).
[13] M. A. Nielsen and I. L. Chuang, *Quantum Computation and Quantum Information* (Cambridge University Press, London, 2006).
[14] P. Kumar, S. Malinovskaya, and V. Malinovsky, J. Phys. B: At. Mol. Opt. Phys. **44**, 154010 (2011).
[15] P. Kumar and S. Malinovskaya, J. Mod. Opt. **57**, 1243 (2010).
[16] P. Kumar, S. Sharma, and H. Singh, J. Theor. Comput. Chem. **8**, 157 (2009).
[17] H. Singh, S. Sharma, P. Kumar, J. Harvey, and G. G. Balint-Kurti, Lect. Notes Comput. Sci. **5102**, 387 (2008).
[18] M. P. A. Branderhorst, P. Londero, P. Wasylczyk, C. Brif, R. L. Kosut, H. Rabitz, and I. A. Walmsely, Science **320**, 638 (2008).
[19] R. J. Levis, G. M. Menkir, and H. Rabitz, Science **292**, 709 (2001); H. Rabitz, *ibid.* **299**, 525 (2003).
[20] B. Amstrup, R. J. Carlson, A. Matro, and S. A. Rice, J. Phys. Chem. **95**, 8019 (1991).
[21] P. Kumar, S. A. Malinovskaya, I. R. Sola, and V. S. Malinovsky, Mol. Phys. **112**, 326 (2014).
[22] P. R. Berman and V. S. Malinovsky, *Principles of Laser Spectroscopy and Quantum Optics* (Princeton University Press, Princeton, NJ, 2011).
[23] P. Gross, D. Neuhauser, and H. Rabitz, J. Chem. Phys. **96**, 2834 (1992).
[24] M. Artamonov, T.-S. Ho, and H. Rabitz, Chem. Phys. **305**, 213 (2004).
[25] J. Werschnik and E. K. U. Gross, J. Opt. B: Quantum Semiclass. Opt. **7**, S300 (2005).
[26] C. Gollub, M. Kowalewski, and R. de Vivie-Riedle, Phys. Rev. Lett. **101**, 073002 (2008).
[27] P. von den Hoff, S. Thallmair, M. Kowalewski, R. Siemering, and R. de Vivie-Riedle, Phys. Chem. Chem. Phys. **14**, 14460 (2012).
[28] D. Tannor, V. Kazakov, and V. Orlov, in *Time-Dependent Quantum Molecular Dynamics*, edited by J. Broeckhove and L. Lathouwers (Plenum, New York, 1992), p. 347.
[29] J. P. Palao, R. Kosloff, and C. P. Koch, Phys. Rev. A **77**, 063412 (2008).